Front. Mech. Eng. 2022, 17(1): 12
https://doi.org/10.1007/s11465-021-0668-9

RESEARCH ARTICLE

Coupling evaluation for material removal and thermal control on precision milling machine tools

Kexu LAI[a], Huajun CAO (✉)[a], Hongcheng LI[b], Benjie LI[c], Disheng HUANG[a]

[a] *State Key Laboratory of Mechanical Transmissions, Chongqing University, Chongqing 400044, China*
[b] *School of Advanced Manufacturing Engineering, Chongqing University of Posts and Telecommunication, Chongqing 400065, China*
[c] *College of Mechatronic Engineering, Southwest Petroleum University, Chengdu 610500, China*

✉ *Corresponding author. E-mail: hjcao@cqu.edu.cn (Huajun CAO)*

ABSTRACT Machine tools are one of the most representative machining systems in manufacturing. The energy consumption of machine tools has been a research hotspot and frontier for green low-carbon manufacturing. However, previous research merely regarded the material removal (MR) energy as useful energy consumption and ignored the useful energy consumed by thermal control (TC) for maintaining internal thermal stability and machining accuracy. In pursuit of energy-efficient, high-precision machining, more attention should be paid to the energy consumption of TC and the coupling relationship between MR and TC. Hence, the cutting energy efficiency model considering the coupling relationship is established based on the law of conservation of energy. An index of energy consumption ratio of TC is proposed to characterize its effect on total energy usage. Furthermore, the heat characteristics are analyzed, which can be adopted to represent machining accuracy. Experimental study indicates that TC is the main energy-consuming process of the precision milling machine tool, which overwhelms the energy consumption of MR. The forced cooling mode of TC results in a 7% reduction in cutting energy efficiency. Regression analysis shows that heat dissipation positively contributes 54.1% to machining accuracy, whereas heat generation negatively contributes 45.9%. This paper reveals the coupling effect of MR and TC on energy efficiency and machining accuracy. It can provide a foundation for energy-efficient, high-precision machining of machine tools.

KEYWORDS machine tools, cutting energy efficiency, thermal stability, machining accuracy, coupling evaluation

1 Introduction

With the depletion of global energy resources and the release of regulation about energy conservation and emission mitigation, how to use energy effectively has become a major problem. The International Energy Agency pointed out that by 2035, global energy demand will increase by one-third compared with 2010, reaching 16.75 billion tons of oil equivalent [1]. Moreover, the energy consumption in the industrial sector accounts for about 37% of total global energy consumption [2], of which about 70% is used for machining [3]. Machine tool, as the extensively used fundamental equipment, is the main source of energy consumption. According to statistics, China has the largest number of machine tools in the world, and more than 7 million are used in China's machining workshops, which leads to a large energy consumption [4]. However, many previous studies pointed out that the energy efficiency of machine tools is very low, usually less than 30% [5,6]. Therefore, reducing the energy consumption and improving the energy efficiency of machine tools is an urgent issue.

In recent years, enormous efforts have been made to investigate the energy consumption characteristics of machine tools. Gutowski et al. [7] pioneered a machine tool energy consumption model and divided the energy consumption of a machine tool into two parts: variable energy consumption related to material removal (MR) and constant energy consumption of functional parts. Sihag and Sangwan [8] used a systematic methodology to understand the evolution of research in machining energy and proposed a six-level hierarchical model to understand machining energy classification better. Based on information extracted from NC programs, He et al. [9] proposed energy models for fixed energy, coolant pump, spindle motor, and feed motors; the proposed models could help

Received September 11, 2021; accepted November 21, 2021

process planning designers make robust decisions in selecting a more energy-efficient NC program. Liu et al. [10] presented a new energy consumption prediction method of the main driving system, and the proposed method can predict the energy consumption before the actual machining with the basic database of the machine tools, workpiece drawing, and planned process planning. Xie et al. [11] proposed a modeling approach for energy efficiency of machining system that can be used to monitor energy efficiency online and without any extra cutting force dynamometer. Chen et al. [12] presented a comprehensive literature review of energy-efficient cutting parameter optimization and decomposed total energy consumption into the electrical energy consumption of machine tool and the embodied energy of the cutting tool and cutting fluid. From a data-driven perspective, Katchasuwanmanee et al. [13,14] combined the raw machining data and the final performance of quality and efficiency to reduce energy consumption and improve the manufacturing performance of complex machining processes, which has remarkable implications for machine tools to achieve collaborative optimization.

The above studies are substantial to energy consumption modeling of machine tools. However, the previous research primarily referred to the energy consumed by MR and the energy consumption characteristics of thermal control (TC) are rarely studied. With the demand for high-efficiency precision machining, the machine tool is expected to have not only a higher cutting energy efficiency but also a better machining accuracy. An important factor of machining accuracy is the internal thermal stability of the machine tools. A previous study stated that 75% of geometric errors of machined workpieces are caused by thermal errors that occur during machining [15]. Therefore, the TC of machine tools is of great importance to maintaining the thermal stability, and hence the machining accuracy and the accuracy of the machine tools.

Several studies have found that TC is crucial to maintaining the thermal stability of machine tools, and the energy demand of TC is considerably higher than the energy required for MR [16]. Gutowski et al. [7] pointed out that the energy consumption of MR is only about 15% of the total, the remainder is regarded as auxiliary energy consumption, and a large part of the auxiliary energy consumption is used to maintain thermal stability. Moradnazhad and Unver [17] developed the energy consumption model of the turning–milling system; they concluded that the energy used for MR process only accounts for about 6% of total energy, and the remainder may be mainly used to maintain thermal stability of the machine tool. Li et al. [18] considered MR energy consumption and thermal stability control energy consumption as useful energy consumption and proposed an exergy-based method to evaluate the comprehensive energy efficiency of the machine tool.

Traditional energy research is devoted to improving the energy efficiency of machine tools by increasing cutting rate [15]. Okwudire and Rodgers [19] thought the improvement of energy efficiency should not overly sacrifice the thermal stability and the machining accuracy of machine tools. In fact, the increase of cutting rate induces a larger multisource heat generation power that deteriorates the uneven temperature field and finally affects the machining accuracy of the machine tools. As a result, to maintain machining accuracy, more operation time or power consumption of TC units are needed for heat dissipation, which inevitably increases the total energy consumption of the machine tool and reduces cutting energy efficiency. Thus, investigating the coupling relationship of these two processes is of great importance to developing effective strategies for balancing cutting energy efficiency and machining accuracy of machine tools.

Based on the above remarks, the effects of the two functional processes on cutting energy efficiency and machining accuracy are investigated from a theoretical view. A cutting energy efficiency model considering the coupling relationship is established based on the law of conservation of energy. The energy consumption ratio of TC is defined to characterize its influence on total energy consumption. Thermal analysis is used to indicate the influence of the two processes on heat characteristics. Moreover, the heat accumulation model of the machine tool is established to represent the machining accuracy of machine tools. Finally, the influence of the coupling relationship between the two processes on cutting energy efficiency and machining accuracy is explored in the experimental study.

The remainder of this paper is organized as follows. A detailed description of the problem about the coupling relationship between MR and TC of machine tools is presented in Section 2. Afterward, based on the energy and heat characteristic analysis of MR, the cutting energy efficiency model is proposed, heat generation is calculated, and the analysis of the influences on cutting energy efficiency and machining accuracy are presented in Section 3. Similarly, the energy consumption ratio and heat dissipation performances related to TC are analyzed in Section 4, which reveals the influences of TC on cutting energy efficiency and machining accuracy. An experimental study is conducted in Section 5 to verify the established models and explore the coupling relationship between the two processes. Conclusions and future work are given in Section 6.

2 Problem statement

Figure 1 shows the MR and TC of a milling machine tool. MR is directly related to product value addition, and it mainly consists of the driving systems such as spindle

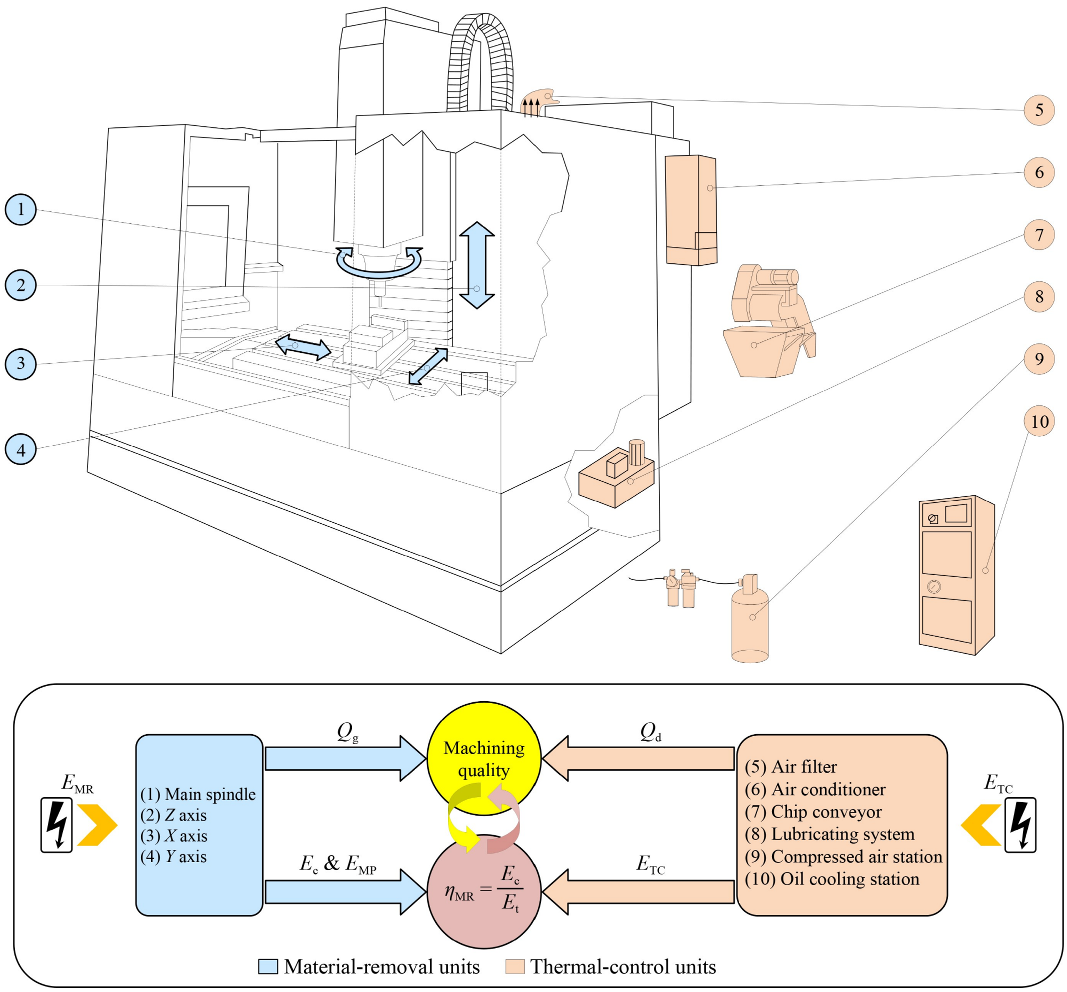

Fig. 1 Functional units of a typical milling machine tool.

unit and feed units. During MR, the electrical energy supplied to the driving systems is converted into mechanical energy for workpiece MR. In previous studies, only the energy consumption for workpiece MR is considered as useful energy consumption, and much attention has been given to the energy efficiency of MR [20,21].

However, due to energy conversion efficiency and friction loss, heat is gradually generated and accumulated in the machine tool with the progress of MR. If the generated heat cannot be taken away in time, the tool service life and the thermal stability and machining accuracy of the machine tool could deteriorate [22–24]. Großmann [25] pointed out a proportional chain between MR power and machining accuracy of the machine tools, as shown in Eq. (1):

$$P_{MR} \propto P_l \propto Q_a \propto \Delta T \propto \Delta L \propto \frac{1}{G_w}, \quad (1)$$

where P_{MR} represents the power consumed by MR, P_l is the power loss related to MR, Q_a is the heat accumulation of the machine tool, ΔT is the temperature rise of a certain component, ΔL is the thermal deformation of a certain component, such as spindle and cutting tool, and G_w is the machining accuracy. An inverse relationship exists between P_{MR} and G_w, that is, a large P_{MR} leads to a poor machining accuracy of the machine tool, which causes geometric errors to machined workpieces.

The main function of TC is to dissipate the generated heat and control the temperature rise and thermal deformation of the machine tool components that can directly affect machining accuracy [15,26]. Like Eq. (1), a proportional chain of the TC process can be defined as Eq. (2):

$$P_{TC} \propto \frac{1}{Q_a} \propto \frac{1}{\Delta T} \propto \frac{1}{\Delta L} \propto G_w, \quad (2)$$

where P_{TC} is the power consumed by TC that is proportional to machining accuracy, that is, TC is beneficial to reducing the heat accumulation and ensuring machining accuracy.

Equation (2) indicates that a large amount of electrical energy is consumed by TC to ensure machining accuracy and accuracy consistence requirements, which has a decisive influence on the overall energy demand of the precision machine tools [27,28]. It inevitably leads to the reduction of cutting energy efficiency η_{MR}.

Therefore, a coupling relationship exists between MR and TC that together affect the energy consumption and heat accumulation of the machine tools and finally influence cutting energy efficiency η_{MR} and machining accuracy G_w. The coupling relationship between the two processes can be briefly presented by Fig. 2. In Fig. 2(a), the curve $P_{MR}-G_w$ illustrates that the higher P_{MR} is, the more heat is generated and the worse G_w is. On the contrary, the curve $P_{TC}-G_w$ shows that a higher P_{TC} can lead to a better heat dissipation performance and G_w. The curve $P_{MR}/P_{TC}-E$ denotes that the higher P_{MR} or P_{TC} is, the more energy is consumed in the same machining time. In Fig. 2(b), the curve $P_{MR}-\eta_{MR}$ shows that the greater P_{MR} is, the higher η_{MR} is when other powers are constant. Conversely, the curve $P_{TC}-\eta_{MR}$ demonstrates that assuming other powers remain unchanged, η_{MR} decreases with the increase of P_{TC} [16].

3 Analysis of MR

3.1 Influence on cutting energy efficiency

The ISO 14955 standard for the environmental evaluation of machine tools defined the energy efficiency as the "ratio or other quantitative relationship between an output of performance, service, goods, or energy, and an input of energy" [29]. According to this definition, cutting energy efficiency η_{MR} can be defined as the ratio of cutting energy used for workpiece MR E_c and the total electrical energy consumption of the machine tool E_t. η_{MR} is calculated, as shown in Eq. (3):

$$\eta_{MR} = \frac{E_c}{E_t}. \tag{3}$$

To calculate the total energy consumption of the machine tool, the characteristics of manufacturing and power variation should be acquainted. Figure 3 shows a power consumption profile of a machine tool during different machining stages. Figure 3 shows that machining consists of several stages, namely, switch on, standby, air cutting, cutting, forced cooling, cutting, and switch off. Three different processes are implemented by the input electrical power, the MR process powered by $P_{MR\text{-}c}$ and P_c ($P_{MR\text{-}c}$ represents the power consumed by MR units during noncutting operation, P_c represents cutting power), the TC process powered by $P_{TC\text{-}s}$ and $P_{TC\text{-}c}$ ($P_{TC\text{-}s}$ indicates the power consumption of TC units during the standby operation, $P_{TC\text{-}c}$ indicates the power consumption of TC units during the cooling operation), and the basic process powered by P_b.

Total energy consumption E_t can be calculated by Eq. (4):

$$E_t = E_{MR} + E_{TC} + E_b, \tag{4}$$

where E_{MR} is the energy consumed by the MR units, used for basic movement and cutting of main spindle and feed axes, E_{TC} is the energy consumed by the TC units such as cooling unit, lubrication unit, and constant-temperature control unit, and E_b is the energy consumed by basic functional units, such as displays, relays, and lights.

E_{MR} is calculated, as shown in Eq. (5):

$$E_{MR} = E_{MR\text{-}c} + E_c, \tag{5}$$

where $E_{MR\text{-}c}$ is the total constant energy requirement of main spindle and feed axes during noncutting stage, and it can be calculated by Eq. (6):

$$E_{MR\text{-}c} = E_{ms} + E_f + E_{tc} = \sum_1^i P_i t_i, \tag{6}$$

where E_{ms} and E_f are energy requirements of the main spindle and the feed motors during noncutting stage, respectively, E_{tc} is the energy requirement of the tool change system, P_i and t_i are the power and the operating time of the ith MR unit, respectively.

Cutting energy is closely related to cutting force and changes with the workpiece materials, tool characteristics, and machining parameters. As a face milling shown in Fig. 4, E_c can be calculated by Eqs. (7) and (8):

$$E_c = \int_0^{t_c} P_c \mathrm{d}t, \tag{7}$$

$$P_c = \frac{F_c v_c}{60 \times 10^4 \eta_m}, \tag{8}$$

where t_c is the cutting time, F_c is the cutting force, v_c is

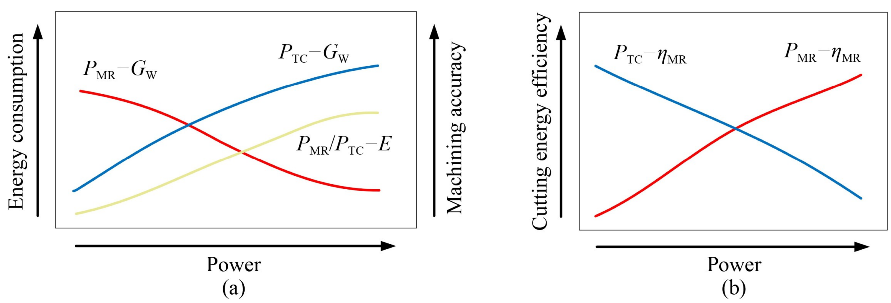

Fig. 2 Coupling relationship between MR and TC. (a) Power versus energy consumption and machining accuracy, (b) power versus cutting energy efficiency.

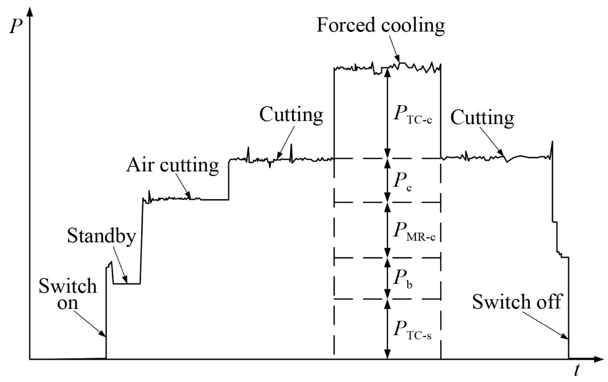

Fig. 3 Power consumption profile of typical milling.

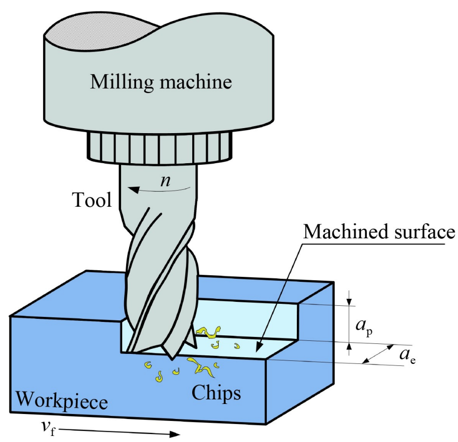

Fig. 4 Typical end milling with a milling cutter.

the cutting speed, and η_m is the spindle motor efficiency.

The mathematic model for the calculation of F_c is shown in Eq. (9):

$$F_c = \frac{C_F {a_p}^{x_F} {a_f}^{y_F} {a_e}^{u_F}}{{d_0}^{q_F} n^{w_F}} k_{F_c}, \tag{9}$$

where C_F, x_F, y_F, u_F, q_F, w_F, and k_{F_c} are several cutting coefficients that can be found in the cutting manual [30], a_p is the depth of cut, a_e is the cutting width, a_f is the feed rate per tooth, d_0 is the diameter of cutting tool, and n is the rotation speed of the main spindle.

For TC units, electricity consumption E_{TC} is the sum of the energy consumption of all TC units in two different working modes (cooling mode and standby mode), and the calculation model is shown in Eq. (10):

$$E_{TC} = \sum_{j=1}^{n} E_{TC\text{-}u}^{j}, \tag{10}$$

where $E_{TC\text{-}u}^{j}$ is the electricity consumption of the jth TC unit.

The power consumption of each basic unit is a constant value. The total energy consumption of all basic units, E_b, is only varied with the operating time and calculated by Eq. (11):

$$E_b = \sum_{k=1}^{n} P_k t_k, \tag{11}$$

where P_k and t_k are the power consumption and the operating time of the kth basic unit, respectively. Therefore, Eq. (1) can be rewritten as Eq. (12):

$$\eta_{MR} = \frac{E_c}{E_t} = \frac{E_c}{E_{MR} + E_{TC} + E_b}. \tag{12}$$

3.2 Influence on machining accuracy

A large amount of heat is generated during MR, which seriously affects the machining accuracy of the machine tools. Thus, several TC strategies are adopted to control the multisource heat generation in the machine tool. During MR, the main heat sources of the machine tool are motors, bearings, moving parts, and cutting area [31]. Figure 5 shows that taking the electric spindle of a precision milling machine tool as an example, the high-speed rotation of spindle bearings leads to friction heat generation. Moreover, due to the poor heat dissipation condition, the power loss of the spindle built-in motor causes intensive heat generation and accumulation that remarkably affect spindle machining accuracy [32]. To eliminate the heat generated inside the electric spindle, several strategies are adopted, such as supplying compressed air into the spindle and designing circulating cooling grooves around the stator and bearing housings.

Previous researchers pointed out that the power loss of main spindle system P_l^{ms} is mainly converted into heat generation $\dot{Q}_g^{ms}$, and power loss consists of power loss of amplifier P_l^a, power loss of inner motor P_l^{im}, and power loss of mechanical transmission chains P_l^{mf} [20,32]. Therefore, $\dot{Q}_g^{ms}$ can be calculated by Eq. (13). For the feed system, heat generation has a similar calculation model.

$$\dot{Q}_g^{ms} = P_l^{ms} = P_l^a + P_l^{im} + P_l^{mf}. \tag{13}$$

Cutting zone is another critical heat source. Figure 6 shows a principle diagram of workpiece MR. According to metal cutting theory [34,35], cutting heat generation occurs in three deformation zones: (1) primary (shear plane), (2) secondary (chip and rake face contact area), and (3) tertiary (flank face and transition surface contact area). Compressed air is widely used to remove cutting heat during dry machining.

Almost all the cutting energy is converted into cutting heat Q_c, which is transferred to cutting tool Q_t, chip Q_{ch}, and workpiece Q_{wp} (the arrows in Fig. 6 represent the heat transfer). According to Ref. [36], cutting heat can be calculated by Eq. (14):

$$Q_c = \eta F_c v_c, \tag{14}$$

where η represents the conversion efficiency of mechanical energy to heat, and its value can be found in Ref. [34]. The generation and transfer of cutting heat aggravate the tool wear and the uneven temperature rise of the machine tool structure, which finally affects tool service life and machining accuracy.

4 Analysis of TC

4.1 Influence on cutting energy efficiency

Equation (12) shows that the increase of TC energy consumption decreases cutting energy efficiency η_{MR}. Compared with the conventional machine tools, precision machine tools consume more electrical energy for thermal stability control and have a lower cutting energy efficiency. To characterize how much energy is consumed by TC, an index of energy consumption ratio η_{TC} is defined as the ratio of electrical energy consumed by the TC units and the total energy consumption of the machine tools E_{t}. The mathematical model of the energy consumption ratio of the TC process is expressed in Eq. (15):

$$\eta_{\mathrm{TC}} = \frac{E_{\mathrm{TC}}}{E_{\mathrm{t}}} = \frac{\sum_{i=1}^{n} E_{\mathrm{TC\text{-}u}}^{j}}{E_{\mathrm{t}}}. \tag{15}$$

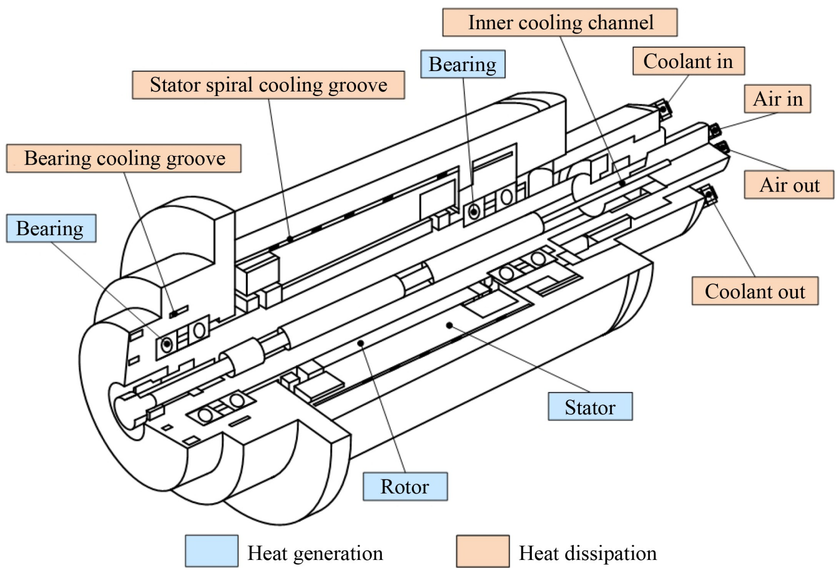

Fig. 5 Heat generation and dissipation of main spindle.

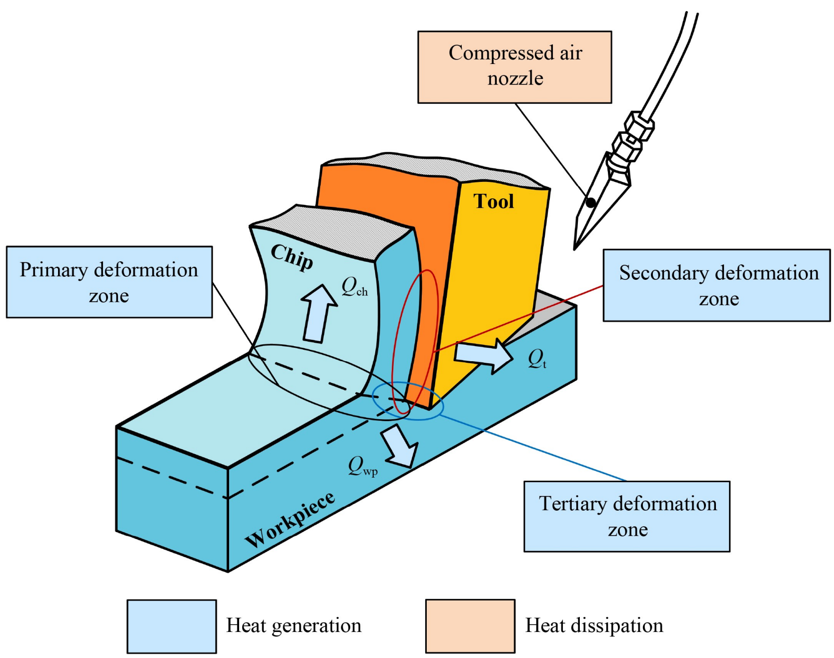

Fig. 6 Heat generation and dissipation of cutting area.

The relationship between electricity consumption $E^{j}_{\text{TC-u}}$ and the heat taken away by each of the TC units can be defined as Eq. (16):

$$COP^{j} = \frac{Q^{j}_{\text{d}}}{E^{j}_{\text{TC-u}}}, \tag{16}$$

where Q^{j}_{d} is the heat taken away by the jth TC unit, and COP^{j} is the coefficient of performance (COP) of the jth TC unit, which is used to characterize the energy conversion efficiency of the TC devices. A higher COP indicates a lower electricity consumption of the TC unit for removing unit heat [37].

4.2 Influence on machining accuracy

In general, the heat dissipation of TC is achieved by circulating the auxiliary mediums in the TC units, such as compressed air, coolant, lubrication, and hydraulic oil. Compressed air is prepared by the air compression station and supplied into the machine tool through one or more nozzles. The heat taken away by compressed air Q^{ca}_{d} can be calculated by Eq. (17):

$$Q^{\text{ca}}_{\text{d}} = \sum_{1}^{n_1} \int_{0}^{t_{\text{A}}} c_{\text{A}} \dot{m}_{\text{A}} (T_{\text{s}} - T_{\text{out}})\,\text{d}t, \tag{17}$$

where n_1 is the number of nozzles, t_{A} is the usage time of compressed air, c_{A} is the specific heat capacity of compressed air, $\dot{m}_{\text{A}}$ is the mass flow rate of compressed air, T_{out} is the air temperature at corresponding nozzle, and T_{s} is the temperature inside the machine tools.

For the hot air pumped out by the air filter, heat dissipation Q^{ha}_{d} can be calculated by Eq. (18):

$$Q^{\text{ha}}_{\text{d}} = \int_{0}^{t_{\text{ha}}} c_{\text{A}} \dot{m}_{\text{ha}} (T_{\text{ha}} - T_{\text{a}})\,\text{d}t, \tag{18}$$

where t_{ha} is the duration time of the hot air flowing into the air filter, $\dot{m}_{\text{ha}}$ is the mass flow rate of the hot air flowing into the electrostatic air filter, T_{ha} is the temperature of hot air, whose value is equal to T_{s}, and T_{a} is ambient temperature.

For the auxiliary liquid mediums, such as coolant, lubricant, and hydraulic oil, the general calculation of heat dissipation (Q^{li}_{d}) is shown in Eq. (19):

$$Q^{\text{li}}_{\text{d}} = \int_{0}^{t_{\text{li}}} c_{\text{li}} \dot{m}_{\text{li}} (T_{\text{li,out}} - T_{\text{li,in}})\,\text{d}t, \tag{19}$$

where t_{li} is the duration time of auxiliary liquid, c_{li} is the specific heat capacity of auxiliary liquid, $\dot{m}_{\text{li}}$ is the mass flow rate of auxiliary liquid, $T_{\text{li,out}}$ is the output temperature of auxiliary liquid, and $T_{\text{li,in}}$ is the input temperature of auxiliary liquid.

Combining with Eqs. (13), (14), and (17)–(19), the heat accumulation of the machine tool can be expressed as Eq. (20). Therefore, the greater the heat taken away by TC Q_{d} is, the less heat is accumulated in machine tool, Q_{a}, which is beneficial to machining accuracy G_{w}.

$$Q_{\text{a}} = Q_{\text{g}} - Q_{\text{d}}, \tag{20}$$

where Q_{g} is the total heat generation of all heat sources.

5 Experimental study

5.1 Experimental setup and design

Experiments are performed on a BV8H type three-axis precision milling machine tool manufactured by the BOCHI Machine Tool Group Co., Ltd., China. The milling cutter with four flutes (z = 4, z represents the tooth number of milling cutter) is manufactured by high-speed steel material, the workpiece material is QT500, and the size is 80 mm × 80 mm × 30 mm. Under actual production condition, the power of the preparation of compressed air is 750 W, and the power and the cooling capacity of the oil cooling station are 1490 and 1500 W, respectively (COP of the oil cooling station is 1.01). The power and the cooling capacity of the air conditioner are 200 and 320 W, respectively (COP of the air conditioner is 1.6). The pressure of the pneumatic system is 0.6 MPa, and the flow rate of the coolant is 50 L/min. Cutting speed v_{c}, feed per tooth a_{f}, and depth of cut a_{p} are selected as the variable parameters, and the designed parameters are shown in Table 1. Based on the orthogonal experiment design method, nine groups of orthogonal experiments with three factors and three levels are designed, as shown in Table 2.

Figure 7 shows the tool path in the milling experiments. The cutter moves from the starting point and removes the

Table 1 Cutting parameters and their levels

Level	Cutting speed, v_{c}/(m·min^{-1})	Feed per tooth, a_{f}/(mm·z^{-1})	Depth of cut, a_{p}/mm
1	15	0.05	0.5
2	18	0.10	1.0
3	21	0.15	1.5

Note: mm·z^{-1} represents feed per tooth.

Table 2 Detailed information of orthogonal experiments

Experimental group	v_{c}/(m·min^{-1})	a_{f}/(mm·z^{-1})	a_{p}/mm
1	15	0.05	0.5
2	18	0.10	0.5
3	21	0.15	0.5
4	18	0.05	1.0
5	21	0.10	1.0
6	15	0.15	1.0
7	21	0.05	1.5
8	15	0.10	1.5
9	18	0.15	1.5

Note: mm·z^{-1} represents feed per tooth.

excess material from the positive to the negative direction along the X axis. After 15 times of cutting, the first layer is removed.

The experimental setup and measurement devices are shown in Fig. 8. A Victor 500 power type power quality analyzer was used to measure the total power consumption characteristics of the machine tool, and PT100 type thermocouples were applied to measure the temperature rise characteristics. Temperature data were collected by an OMEGA OM-DAQ-USB-2400 data acquisition system and recorded by a laptop. The flatness error (δ_{FE}, a kind of geometric error) of the machined workpiece was selected as an indicator to evaluate the machining accuracy of the machine tool, and its value can be calculated from the measured results by a dial gauge (three-point measurement method was applied).

5.2 Results and discussion

5.2.1 Energy consumption and cutting energy efficiency

The power profile of the machine tool under the adoption of the fourth group parameters (a_p = 1 mm, a_f = 0.05 mm/z, v_c = 18 m/min) is shown in Fig. 9. In the removing a single layer of workpiece material, the machine tool experiences power on, standby, material removing, and

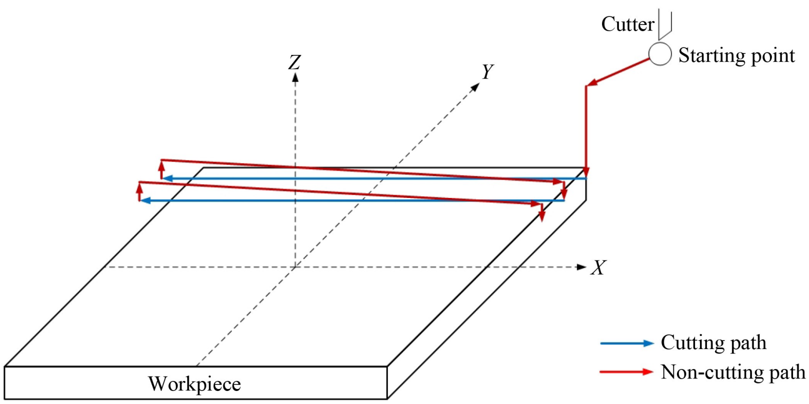

Fig. 7 Trajectory of the cutting tool during cutting process.

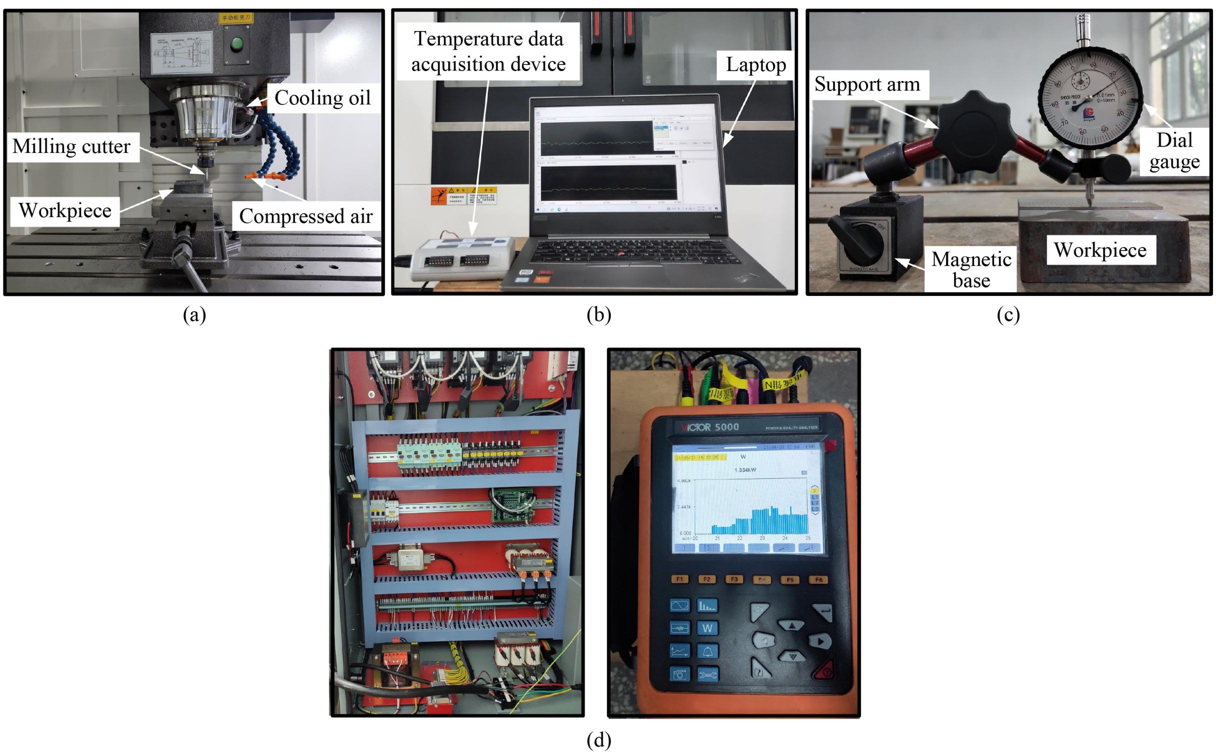

Fig. 8 Milling experimental setup: (a) milling cutter and workpiece, (b) temperature data acquisition device and laptop, (c) dial gauge, (d) power bus of the machine tool (left), power and quality analyzer (right).

power off. Figure 9 shows that the power of the TC-standby process accounts for 20.2%, and the cooling power of the TC process accounts for 32.5%. During a certain period of machine operation, more than 50% (cooling power $P_{TC\text{-}c}$ plus standby power $P_{TC\text{-}s}$) of the electricity consumption is used to control the internal thermal stability of the machine tool.

Combining measured power and temperature data, total energy consumption E_t, MR energy consumption E_c, TC energy consumption E_{TC}, and the corresponding η_{MR} and η_{TC} can be calculated. The calculated results are shown in Fig. 10. The three types energy consumption in the first group of cutting parameters have the maximum values (with the longest cutting time), and the third group has the smallest values (with the shortest cutting time). The line in Fig. 10 reflects the proportion of electrical energy consumed by TC and MR. The energy consumption of TC accounts for 32%–36% of total energy consumption, which is the main energy consumption of the machine tool and is much larger than the one consumed by cutting (accounting for 17%–20% of total energy consumption).

Heat accumulation results in temperature rise. When temperature reaches the threshold, the working state of TC units is automatically changed from standby mode (ordinary refrigeration) to cooling mode (forced refrigeration), which results in a decrease of cutting energy efficiency. Figure 11 shows the change of cutting energy efficiency before and after the cooling mode. Cutting energy efficiency η_{MR} is reduced by approximately 7% after the cooling mode is on, and the reduction rate is approximately 33%, which indicates that TC has a remarkable influence on cutting energy efficiency η_{MR}.

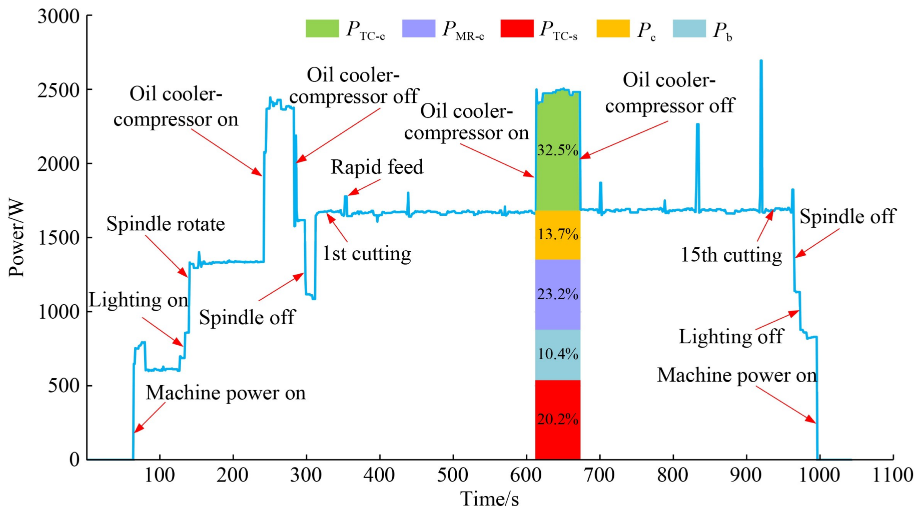

Fig. 9 Power consumption profile of the 4th group during different operation stages.

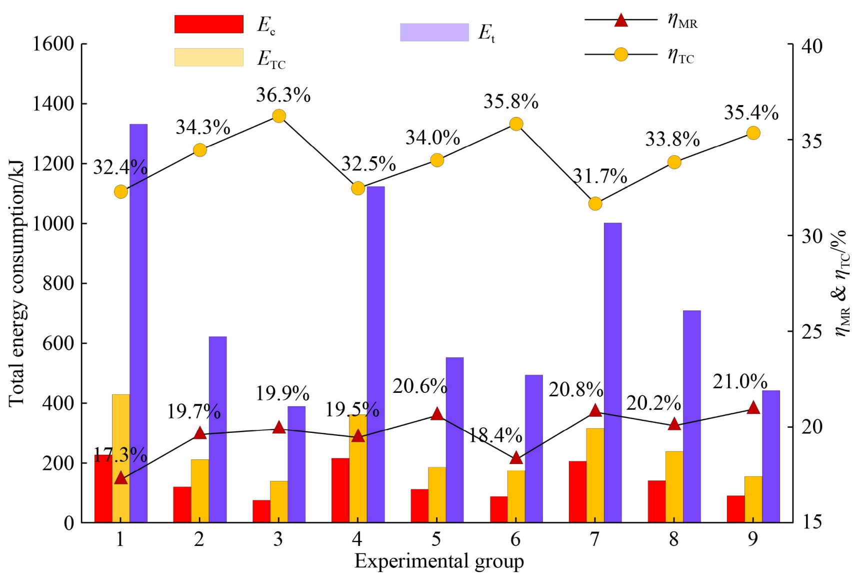

Fig. 10 Composition and proportion of total energy consumption.

5.2.2 Heat characteristics and flatness error

According to Eqs. (13) and (14), the heat generated by MR can be calculated. The results show that 20% of electrical energy input to MR units is converted into heat, and 90% of cutting power is converted into heat. According to Eqs. (17)–(20), heat dissipation and heat accumulation can be calculated. Details of heat characteristics and flatness errors can be seen in Fig. 12.

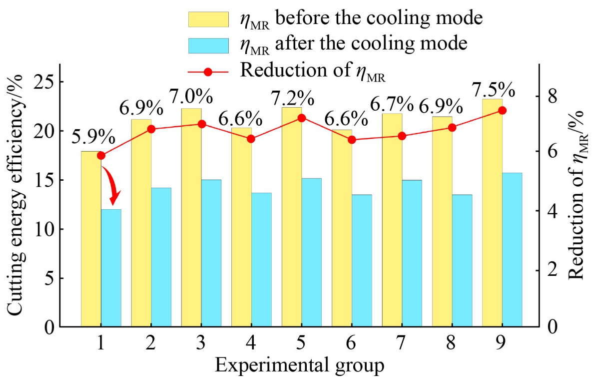

Fig. 11 Change of η_{MR} before and after the cooling mode.

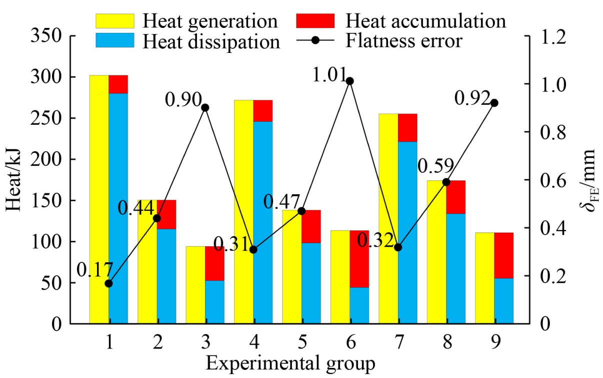

Fig. 12 Heat characteristics and flatness error of each experimental group.

Figure 12 shows that the change trends of heat generation and heat dissipation are similar to total energy consumption, that is, the more electrical energy the machine tool consumes, the greater the heat generated by MR and the greater the heat dissipated by TC. In addition, the greater the heat accumulation is, the greater the flatness error δ_{FE} of the machined workpieces and the worse the machining accuracy of the machine tool.

Owing to the linear relationship between heat and flatness error, multiple linear regression is used to calculate flatness error δ_{FE}, the expression is shown as Eq. (21), and the square value of the fitting correlation coefficient (R^2) is 0.888. The effect coefficient of Q_d is negative (-1.18^{-5}), which means heat dissipation has a negative influence on flatness error.

$$\delta_{FE} = 1.01^{-5} Q_g - 1.18^{-5} Q_d. \tag{21}$$

The contributions of Q_g and Q_d to δ_{FE} are calculated as 45.9% and 54.1%, respectively, which indicate that heat dissipation Q_d is more influential to flatness error than heat generation Q_g. Therefore, the method of increasing TC power P_{TC} and increasing heat dissipation Q_d is more helpful to improving machining accuracy than the method of reducing MR power P_{MR} and reducing heat generation Q_g.

5.2.3 Relationships between energy consumption, cutting energy efficiency, and machining accuracy

To achieve more sustainable machining processes, minimizing the total energy consumption of the machining tools is desired. Moreover, cutting energy efficiency and machining accuracy are of great importance for machining that should not be ignored.

Figure 13 shows the relationship of total energy consumption, cutting energy efficiency, and machining accuracy under different cutting parameters. Figure 13(a) shows that a higher cutting energy efficiency can be obtained by selecting large cutting parameters (fifth,

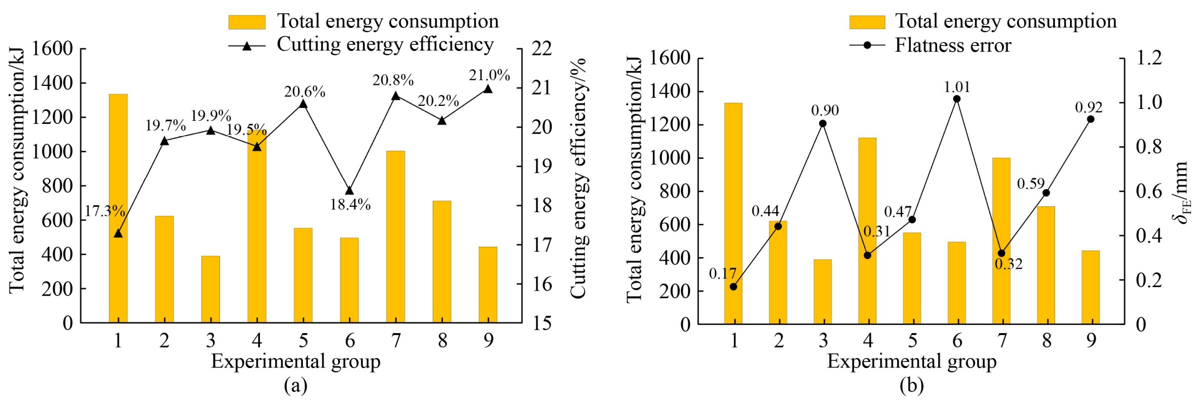

Fig. 13 Comprehensive comparisons in energy consumption, cutting energy efficiency, and machining accuracy: (a) total energy consumption and cutting energy efficiency, (b) energy consumption and flatness error.

seventh, and ninth experiments). Moreover, selecting a large feed rate can substantially reduce cutting time, thereby reducing $E_{\text{MR-c}}$ of MR and $E_{\text{TC-s}}$ of TC, which finally reduces total energy consumption. Therefore, when pursuing a high cutting energy efficiency and a low total energy consumption, larger cutting parameters can be selected, such as the ninth group experiment.

Figure 13(b) shows that the machining accuracy in the first group is the best (with the smallest δ_{FE}) because all the cutting parameters in the first group are minimum, resulting in the smallest cutting power and the smallest cutting heat per unit time, which allows the TC units in the standby state to take away the heat generated by MR in time, thereby reducing heat accumulation. The sixth group experiment has the largest flatness error because its cutting time is very short, and the forced cooling of TC only operates in a short time before completing machining, which leads to heat accumulation and causes machining accuracy to worsen. Therefore, when pursuing a high machining accuracy and a low energy consumption, medium cutting parameters can be selected, such as the second and fifth experimental groups.

The above experimental data are drawn into a 3D surface map, as shown in Fig. 14, where the vertical axis represents E_{t}, and the curve represents the isoline of energy consumption. A higher machining accuracy (with a smaller δ_{FE}) corresponds to a higher E_{t} because to ensure machining accuracy, more E_{TC} is needed to take away the heat generated by MR. The result illustrated in Fig. 14 is from the limited experimental data and cannot reflect deeply the dynamic characteristics of the process. Therefore, no clear relationship exists between η_{MR} and E_{t}, and η_{MR} and δ_{FE} in the figure. The connection depends on the dynamic energy and thermal characteristics influenced by the interaction between MR and TC, which is a key issue that will be explored in the future.

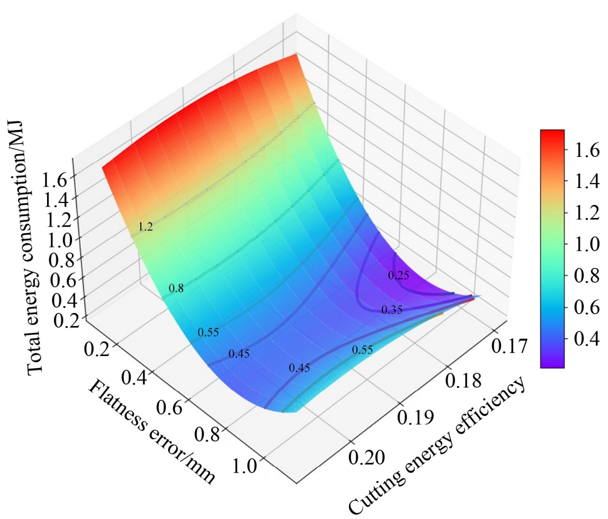

Fig. 14 3D surface map of energy consumption, cutting energy efficiency, and flatness error.

6 Conclusions

As a key equipment of the manufacturing industry, the precision milling machine should meet not only the requirement of energy efficiency but also machining accuracy. The two requirements are implemented by two coupled processes, namely, MR and TC. More specifically, the energy consumed by MR for value addition and the energy used by TC to maintain internal thermal stability and ensure machining accuracy together affect total energy consumption and cutting energy efficiency. Moreover, the heat generation of MR and the heat dissipation of TC have great influences on machining accuracy.

In this paper, based on the law of conversation of energy, the cutting energy efficiency model is proposed, and the energy consumption ratio related to TC is defined. The influences on cutting energy efficiency of the two processes are also analyzed by energy characteristics. Subsequently, the heat generation of MR and the heat dissipation of TC are analyzed according to the knowledge of thermodynamics, where the heat characteristics directly affect machining accuracy. Finally, an experimental study is conducted to demonstrate the feasibility of the proposed models, and the trade-off relationships between total energy consumption, cutting energy efficiency, and machining accuracy are investigated.

This paper reveals the coupling relationship between MR and TC of precision milling machine tool. TC accounts for 32%–36% of total energy consumption, which dominates the energy consumption of the precision machine tool compared with MR. Moreover, the energy consumption of TC plays a substantial role in cutting energy efficiency, which can reduce cutting energy efficiency by 7% after the cooling mode is on. Furthermore, the heat characteristics resulting from MR and TC have important effects on machining accuracy. Compared with the 45.9% negative contribution of MR, TC has a 54.1% of positive contribution to machining accuracy.

Based on this paper, future work can consider investigating the energy efficiency characteristics in a dynamic thermal environment. Another work is to optimize MR and TC for balancing machining accuracy and energy efficiency.

Nomenclature

a_{e}	Cutting width
a_{f}	Feed rate per tooth
a_{p}	Depth of cut
c_{A}	Specific heat capacity of compressed air

c_{li}	Specific heat capacity of auxiliary liquid
C_F, x_F, y_F, u_F, q_F, w_F, and k_{F_c}	Cutting coefficients
COP^j	Coefficient of performance of the jth TC unit
d_0	Diameter of cutting tool
E_b	Energy consumed by basic functional units
E_c	Cutting energy
E_f	Energy requirements of feed motors during noncutting stage
E_{ms}	Energy requirement of the main spindle during noncutting stage
E_{MR}	Energy consumed by MR units
$E_{MR\text{-}c}$	Constant energy requirement of main spindle and feed axes during noncutting stage
E_{tc}	Energy requirement of the tool change system
E_t	Total energy consumption of machine tool
E_{TC}	Energy consumed by TC units
$E_{TC\text{-}u}^j$	Electricity consumption of the jth TC unit
F_c	Cutting force
G_w	Machining accuracy
ΔL	Thermal deformation of a certain component
$\dot{m}_A$	Mass flow rate of compressed air
$\dot{m}_{li}$	Mass flow rate of auxiliary liquid
$\dot{m}_{ha}$	Mass flow rate of the hot air flowing into the electrostatic air filter
n	Rotation speed of the main spindle
n_1	Number of nozzles
P_b	Power of basic operation
P_c	Cutting power
P_i	Power of the ith MR unit
P_k	Power consumption of the kth basic unit
P_l	Power loss related to MR
P_l^a	Power loss of amplifier
P_l^{im}	Power loss of inner motor
P_l^{mf}	Power loss of mechanical transmission chains
P_{MR}	Power consumed by MR
$P_{MR\text{-}c}$	Power consumed by MR units during noncutting operation
P_{TC}	Power consumed by TC
$P_{TC\text{-}c}$	Power consumed by TC units during cooling operation
$P_{TC\text{-}s}$	Power consumed by TC units during standby operation
Q_c	Cutting heat
Q_{ch}	Heat transferred to chips
Q_d	Heat dissipation of machine tool
Q_d^{ca}	Heat taken away by compressed air
Q_d^{ha}	Heat dissipation of hot air
Q_d^j	Heat taken away by the jth TC unit
Q_d^{li}	Heat taken away by auxiliary liquid
Q_g	Heat generation of all heat sources
$\dot{Q}_g^{ms}$	Heat generation of main spindle system
Q_t	Heat transferred to cutting tool
Q_{wp}	Heat transferred to workpiece
t_c	Cutting time
t_{ha}	Duration time of hot air
t_i	Operating time of the ith MR unit
t_k	Operating time of the kth basic-unit
t_{li}	Duration time of auxiliary liquid
t_A	Usage time of compressed air
T_a	Ambient temperature
T_{ha}	Temperature of hot air
$T_{li,in}$	Input temperature of auxiliary liquid
$T_{li,out}$	Output temperature of auxiliary liquid
T_{out}	Air temperature at corresponding nozzle
T_s	Temperature inside machine tool
ΔT	Temperature rise of a certain component
v_c	Cutting speed
z	Tooth number of milling cutter
η	Convert efficiency of mechanical energy to heat
η_m	Spindle motor efficiency
η_{MR}	Cutting energy efficiency
η_{TC}	Energy consumption ratio of TC
δ_{FE}	Flatness error

Acknowledgements This work was supported by the National Natural Science Foundation of China (Grant Nos. 51975076 and 52105533). The authors gratefully acknowledge the reviewers and the editors for their insightful comments.

References

1. Khatib H. IEA world energy outlook 2010—a comment. Energy Policy, 2011, 39(5): 2507–2511
2. Park C W, Kwon K S, Kim W B, Min B K, Park S J, Sung I H, Yoon Y S, Lee K S, Lee J H, Seok J. Energy consumption reduction technology in manufacturing—a selective review of policies, standards, and research. International Journal of Precision Engineering and Manufacturing, 2009, 10(5): 151–173
3. Cai W, Liu C H, Lai K H, Li L, Cunha J, Hu L K. Energy performance certification in mechanical manufacturing industry: a review and analysis. Energy Conversion and Management, 2019, 186: 415–432
4. Cai W, Lai K H. Sustainability assessment of mechanical manufacturing systems in the industrial sector. Renewable and Sustainable Energy Reviews, 2021, 135: 110169
5. Wang Q L, Liu F, Li C B. An integrated method for assessing the energy efficiency of machining workshop. Journal of Cleaner Production, 2013, 52: 122–133

6. Mouzon G, Yildirim M B, Twomey J. Operational methods for minimization of energy consumption of manufacturing equipment. International Journal of Production Research, 2007, 45(18−19): 4247–4271
7. Gutowski T, Dahmus J, Thiriez A. Electrical energy requirements for manufacturing processes. In: Proceedings of the 13th CIRP International Conference on Life Cycle Engineering. Leuven: CIRP, 2006, 623–628
8. Sihag N, Sangwan K S. A systematic literature review on machine tool energy consumption. Journal of Cleaner Production, 2020, 275: 123125
9. He Y, Liu F, Wu T, Zhong F P, Peng B. Analysis and estimation of energy consumption for numerical control machining. Proceedings of the Institution of Mechanical Engineers, Part B: Journal of Engineering Manufacture, 2012, 226(2): 255–266
10. Liu F, Xie J, Liu S. A method for predicting the energy consumption of the main driving system of a machine tool in a machining process. Journal of Cleaner Production, 2015, 105: 171–177
11. Xie J, Cai W, Du Y B, Tang Y, Tuo J B. Modelling approach for energy efficiency of machining system based on torque model and angular velocity. Journal of Cleaner Production, 2021, 293: 126249
12. Chen X Z, Li C B, Tang Y, Li L, Li H C. Energy efficient cutting parameter optimization. Frontiers of Mechanical Engineering, 2021, 16(2): 221–248
13. Li P L, Cheng K, Jiang P Y, Katchasuwanmanee K. Investigation on industrial dataspace for advanced machining workshops: enabling machining operations control with domain knowledge and application case studies. Journal of Intelligent Manufacturing, 2022, 33(1): 103−119
14. Katchasuwanmanee K, Bateman R, Cheng K. Development of the energy-smart production management system (e-ProMan): a big data driven approach, analysis and optimisation. Proceedings of the Institution of Mechanical Engineers, Part B: Journal of Engineering Manufacture, 2016, 230(5): 972–978
15. Mayr J, Jedrzejewski J, Uhlmann E, Donmez M A, Knapp W, Härtig F, Wendt K, Moriwaki T, Shore P, Schmitt R, Brecher C, Würz T, Wegener K. Thermal issues in machine tools. CIRP Annals-Manufacturing Technology, 2012, 61(2): 771–791
16. Denkena B, Abele E, Brecher C, Dittrich M A, Kara S, Mori M. Energy efficient machine tools. CIRP Annals, 2020, 69(2): 646–667
17. Moradnazhad M, Unver H O. Energy consumption characteristics of turn-mill machining. The International Journal of Advanced Manufacturing Technology, 2017, 91(5−8): 1991–2016
18. Li B J, Cao H J, Hon B, Liu L, Gao X. Exergy-based energy efficiency evaluation model for machine tools considering thermal stability. International Journal of Precision Engineering and Manufacturing: Green Technology, 2021, 8(2): 423–434
19. Okwudire C, Rodgers J. Design and control of a novel hybrid feed drive for high performance and energy efficient machining. CIRP Annals: Manufacturing Technology, 2013, 62(1): 391–394
20. Wang Q L, Liu F. Mathematical model of multi-source energy flows for CNC machine tools. Journal of Mechanical Engineering, 2013, 49(7): 5−12 (in Chinese)
21. Wen L, Zein A, Kara S, Herrmann C. An investigation into fixed energy consumption of machine tools. In: Proceedings of the 18th CIRP International Conference on Life Cycle Engineering. Leuven, 2011, 268–273
22. Yang X, Cao H J, Zhu L B, Li B J. A 3D chip geometry driven predictive method for heat-loading performance of hob tooth in high-speed dry hobbing. The International Journal of Advanced Manufacturing Technology, 2017, 93(5−8): 1583–1594
23. Zhu L B, Cao H J, Zeng D, Yang X, Li B J. Multi-variable driving thermal energy control model of dry hobbing machine tool. The International Journal of Advanced Manufacturing Technology, 2017, 92(1−4): 259–275
24. Cao H J, Zhu L B, Li X G, Chen P, Chen Y P. Thermal error compensation of dry hobbing machine tool considering workpiece thermal deformation. The International Journal of Advanced Manufacturing Technology, 2016, 86(5−8): 1739–1751
25. Großmann K. Thermo-energetic Design of Machine Tools. Berlin: Springer International Publishing, 2015
26. Zailani Z A, Hamidon R, Hussin M S, Hamzas M F M A, Hadi H. The influence of solid lubricant in machining parameter of milling operation. International Journal of Engineering Science and Technology, 2011, 3(6): 5221–5226
27. Brecher C, Jasper D, Fey M. Analysis of new, energy-efficient hydraulic unit for machine tools. International Journal of Precision Engineering and Manufacturing-Green Technology, 2017, 4(1): 5–11
28. Zhao G Y, Liu Z Y, He Y, Cao H J, Guo Y B. Energy consumption in machining: classification, prediction, and reduction strategy. Energy, 2017, 133: 142–157
29. ISO. Machine tools—environmental evaluation of machine tools—Part 1: design methodology for energy-efficient machine tools. 2017. Available at ISO website
30. Walsh R A. Handbook of Machining and Metalworking Calculations. New York: McGraw-Hill, 2001, 159–174
31. Fu G Q, Tao C, Xie Y P, Lu C J, Gao H L. Temperature-sensitive point selection for thermal error modeling of machine tool spindle by considering heat source regions. The International Journal of Advanced Manufacturing Technology, 2021, 112(9−10): 2447–2460
32. Denkena B, Bergmann B, Klemme H. Cooling of motor spindles—a review. The International Journal of Advanced Manufacturing Technology, 2020, 110(11−12): 3273–3294
33. Iqbal A, Zhang H C, Kong L L, Hussain G. A rule-based system for trade-off among energy consumption, tool life, and productivity in machining process. Journal of Intelligent Manufacturing, 2015, 26(6): 1217–1232
34. Wu D W. A new approach of formulating the transfer function for dynamic cutting processes. Journal of Engineering for Industry, 1989, 111(1): 37–47
35. Zhu K P, Zhang Y. A generic tool wear model and its application to force modeling and wear monitoring in high speed milling. Mechanical Systems and Signal Processing, 2019, 115: 147–161
36. Yang X, Cao H J, Chen Y P, Zhu L B, Li B J. An analytical model of chip heat-carrying capacity for high-speed dry hobbing based on 3D chip geometry. International Journal of Precision Engineering and Manufacturing, 2017, 18(2): 245–256
37. Kozai T, Sakaguchi S, Akiyama T, Yamada K, Ohshima K. Design and management of PFALs. In: Kozai T, Niu G, Takagaki M, eds. Plant Factory. 2nd ed. Salt Lake City: Academic Press, 2020, 357–375